Substrate binding site flexibility of the small heat shock protein molecular chaperones

Nomalie Jaya, Victor Garcia, and Elizabeth Vierling[1]

Department of Chemistry and Biochemistry, University of Arizona, Tucson, AZ 85721

Edited by George H. Lorimer, University of Maryland, College Park, MD, and approved July 17, 2009 (received for review February 26, 2009)

Small heat shock proteins (sHSPs) serve as a first line of defense against stress-induced cell damage by binding and maintaining denaturing proteins in a folding-competent state. In contrast to the well-defined substrate binding regions of ATP-dependent chaperones, interactions between sHSPs and substrates are poorly understood. Defining substrate-binding sites of sHSPs is key to understanding their cellular functions and to harnessing their aggregation-prevention properties for controlling damage due to stress and disease. We incorporated a photoactivatable cross-linker at 32 positions throughout a well-characterized sHSP, dodecameric PsHsp18.1 from pea, and identified direct interaction sites between sHSPs and substrates. Model substrates firefly luciferase and malate dehydrogenase form strong contacts with multiple residues in the sHSP N-terminal arm, demonstrating the importance of this flexible and evolutionary variable region in substrate binding. Within the conserved α-crystallin domain both substrates also bind the β-strand (β7) where mutations in human homologs result in inherited disease. Notably, these binding sites are poorly accessible in the sHSP atomic structure, consistent with major structural rearrangements being required for substrate binding. Detectable differences in the pattern of cross-linking intensity of the two substrates and the fact that substrates make contacts throughout the sHSP indicate that there is not a discrete substrate binding surface. Our results support a model in which the intrinsically-disordered N-terminal arm can present diverse geometries of interaction sites, which is likely critical for the ability of sHSPs to protect efficiently many different substrates.

alpha-crystallin | cross-linking | intrinsic disorder | P-benzoylphenylalanine | protein–protein interactions

Protein aggregation resulting from stress, disease, or mutation poses a major threat to all cells. Consequently cells have developed mechanisms of "protein quality control" involving specific proteases and molecular chaperones to prevent or resolve protein aggregation (1). The small heat shock proteins (sHSPs) and related vertebrate α-crystallins are ATP-independent molecular chaperones that are ubiquitous components of this protein quality control network. In addition to increased levels of expression during high temperature stress, sHSPs are induced by other stresses (e.g., oxidative stress, heavy metals, ischemic injury) and are constitutive components of certain tissues in many different organisms (2). Expression and/or mutation of specific sHSPs are linked to cancer, neurodegenerative diseases, myopathies, and cataract (3, 4). Furthermore, sHSPs have been suggested to have therapeutic potential for amyotrophic lateral sclerosis (5) and multiple sclerosis (6), and to positively affect longevity in model organisms (7). Defining the mechanism of sHSP chaperone action, therefore, has wide-ranging implications for understanding cellular stress and disease processes.

The sHSPs are defined by a core α-crystallin domain of approximately 100 amino acids, which is flanked by a short C-terminal extension and an N-terminal arm of variable length and divergent sequence (8). The monomeric molecular mass of sHSPs ranges from approximately 12–42 kDa, but in their native state the majority of sHSPs form oligomers of 12 to >32 subunits. X-ray crystal structures are available for two oligomeric sHSPs, the 24-subunit MjHsp16.5 from the archaeon *Methanococcus jannaschii* (9) and the dodecameric *Triticum aestivum* (wheat) TaHsp16.9 (10), both of which are built from a homologous dimer. The N-terminal arms of all subunits of MjHsp16.5 and half of the TaHsp16.9 subunits were unresolved in the crystal structure, and hydrogen-deuterium exchange experiments support a complete lack of stable secondary structure in the N-terminal arms of TaHsp16.9 in solution (11, 12). However, although the N-terminal arm appears to be intrinsically disordered, it cannot be removed without disrupting the TaHsp16.9 dodecamer. The α-crystallin domain comprises an IgG Fc-like β-sandwich with topology identical to the Hsp90 cochaperone p23. The C-terminal extension makes essential contacts that stabilize the oligomeric structure.

sHSPs have an unusually high capacity to bind unfolding proteins and to facilitate subsequent substrate refolding by ATP-dependent chaperone systems (13, 14). Compared with the Hsp90, Hsp70, and GroEL chaperones, however, the mechanism of sHSP substrate binding and chaperone function are poorly defined. Structural and biochemical studies favor a model in which oligomeric sHSPs dissociate into smaller species or undergo structural rearrangement during heat stress (8, 15–18). Hydrophobic surfaces of sHSPs exposed during this structural rearrangement may interact with hydrophobic patches on partially denaturing proteins (8, 14, 19). The substrate-bound sHSPs assemble into large soluble complexes, preventing further aggregation of the denatured proteins (2, 8). Sequence variability and structural disorder, along with experimental evidence make the N-terminal arm a good candidate for substrate binding. Chaperone activity is altered in N-terminal chimeras, and in N-terminal point and deletion mutants, implicating the N-terminal arm in substrate protection (20–23). However, these data do not distinguish between disruption of substrate interaction sites on the N-terminal arm, versus perturbation of some other sHSP property, such as oligomer integrity, which then indirectly impacts chaperone activity. Other data suggest there are additional substrate binding sites on the α-crystallin domain, particularly in certain regions involved in oligomer contacts (10, 14, 24, 25).

How sHSPs can recognize and bind diverse unfolding proteins is key to determining how sHSPs function in vivo and is of fundamental interest to understanding protein aggregation processes. We used site-specific cross-linking to query all domains of dodecameric PsHsp18.1 from pea to identify sHSP-substrate binding sites. PsHsp18.1 is well-characterized biochemically, an extremely effective chaperone, and its structure is readily modeled on that of

Author contributions: N.J. and E.V. designed research; N.J. and V.G. performed research; N.J. and E.V. analyzed data; and N.J. and E.V. wrote the paper.

The authors declare no conflict of interest.

This article is a PNAS Direct Submission.

[1]To whom correspondence should be addressed at: Department of Chemistry and Biochemistry, University of Arizona, 1007 East Lowell Street, Tucson, AZ 85721. E-mail: vierling@u.arizona.edu.

This article contains supporting information online at www.pnas.org/cgi/content/full/0902177106/DCSupplemental.

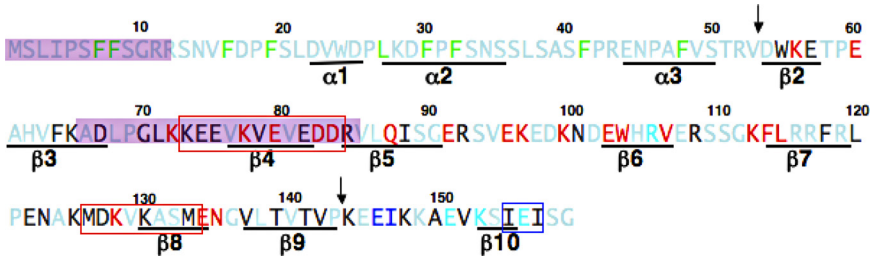

Fig. 1. Sites of Bpa cross-linker incorporation into PsHsp18.1. Positions where Bpa was successfully incorporated into PsHsp18.1 are highlighted: N-terminal arm, green; α-crystallin domain, red; and C-terminal extension, blue. Arrows delimit the α-crystallin domain. Shown in gray and cyan are residues where Bpa incorporation did not yield detectable protein or resulted in unstable protein, respectively. Regions previously implicated in substrate binding are highlighted in purple (14, 19) and boxed in red [one edge of the beta sandwich, which is ''patched'' by the IXI motif in the C-terminal extension (boxed in blue) (10)]. Secondary structure based on TaHsp16.9 (PDB: 1GME) (10).

TaHsp16.9. The UV-activated cross-linker *p*-benzoyl-L-phenylalanine (Bpa) was incorporated into 32 individual sites of PsHsp18.1, and the Bpa-containing variants were complexed with heat-denatured model substrates, malate dehydrogenase (MDH) and firefly luciferase (Luc). The pattern of sHSP cross-linking to these two substrates reveals important principles of substrate recognition by these ubiquitous chaperones.

Results

Strategy To Identify sHSP-Substrate Interaction Sites. To identify regions of sHSPs that directly interact with denaturing substrates, we generated single-site variants of PsHsp18.1 in which the phenylalanine (Phe) analog, Bpa (26), was incorporated at specific positions throughout the protein. Upon UV exposure, Bpa acts as a zero-length cross-linker inserting into a C-H or N-H bond in the immediate vicinity of the probe.

Multiple sites in each structural region of PsHsp18.1, the N-terminal arm (1–53 aa), α-crystallin domain (54–143 aa), and C-terminal extension (144–158 aa) were chosen for probe incorporation (Fig. 1). All Phe residues were substituted, because the structural similarity of Phe and Bpa suggested a minimal disruption of sHSP structure. Selected additional hydrophobic residues and certain charged residues predicted to be on the exterior of the PsHsp18.1 dodecamer and dimer (modeled on TaHsp16.9) were also substituted to achieve distribution of cross-linker throughout the protein. Of a total of 72 substitutions attempted, 32 yielded high levels of recombinant protein, while 36 showed no significant expression and four produced unstable protein which readily degraded (Fig. 1). It is notable that all eight Phe residues in the N-terminal arm tolerated substitution with Bpa, and therefore only one additional Leu residue was substituted in this domain. In contrast, it was difficult to introduce Bpa into the α-crystallin domain, even at Phe sites, presumably because of the packing of the β-sandwich, and the majority of successful substitutions were in charged residues. Two Bpa substitutions were successful in the C-terminal domain. In total, the largest spacing between substitutions was 12 residues, with most significantly closer, achieving excellent coverage of the protein for testing substrate interactions (Fig. 1).

Oligomer Stability of Bpa Variants of PsHsp18.1. All 32 PsHsp18.1 Bpa variants were purified as previously described (27). The oligomeric structure and stability of each variant were examined by size exclusion chromatography (SEC) at room temperature. Seven of the nine Bpa variants in the N-terminal arm behaved like wild type on SEC, consistent with normal dodecameric structure. Interestingly, incorporation of Bpa at F16 and F19 resulted in unstable oligomers, with only a small portion eluting as a dodecamer, some as a dimer, and the remainder as larger oligomers, most of which did not enter the column (Fig. 2*A* and Table S1). The Phe residues at equivalent positions in TaHsp16.9 are involved in oligomer contacts suggesting that the benzoyl group introduces steric strain leading to oligomer instability in these N-terminal variants (10). Of the 21 Bpa variants in the α-crystallin domain, 13 showed normal dodecameric behavior and three others were primarily dodecameric as assessed by SEC (Table S1). The remaining six (K56, Q87, K96, E102, W103, and F113) were unstable dodecamers with both smaller (dimer) and higher molecular weight forms (Fig. 2*A* and Table S1). These variants are likely unstable because they are involved in oligomeric contacts (e.g., K56), or because they disrupt the α-crystallin domain β-sandwich (e.g., Q87, F113). The two C-terminal substitutions yielded one normal dodecamer (E145) and one with a higher molecular weight form (I146). Altogether, behavior of the Bpa variants is consistent with structural features of PsHsp18.1 as modeled on the closely related TaHsp16.9 (10).

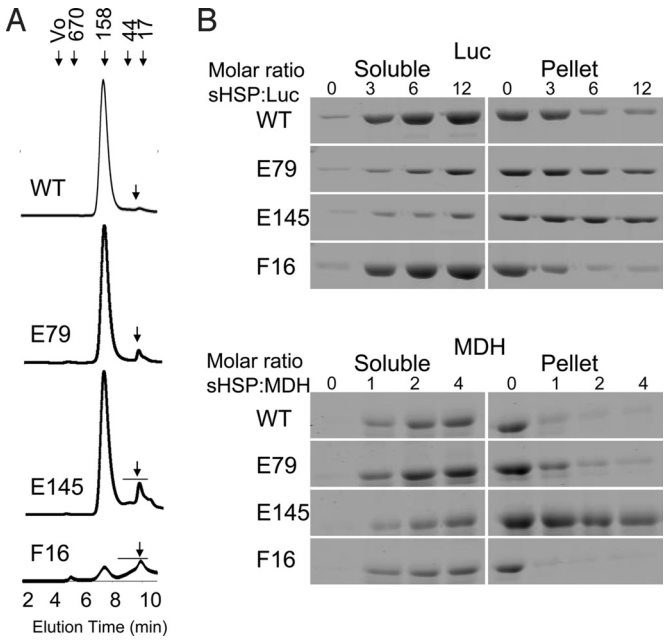

Fig. 2. Dodecamer stability and chaperone activity of selected PsHsp18.1 Bpa variants. (*A*) SEC was used to determine the stability of the native structure of PsHsp18.1 Bpa variants at room temperature. Each protein (100 μL of 12 μM) was injected into the column. (*A*) shows wild-type PsHsp18.1, a dodecamer with a retention time of 7.4 min. The peak at 10 min (arrow) is a minor buffer peak found in all chromatograms. A dimeric species elutes at 8–10 min (line with arrow). E79, E145 and F16 are shown as representative Bpa variants. The majority of F16 behaves as a high molecular weight species retained by the prefilter and never enters the SEC column. (*B*) shows the ability of the same Bpa variants to protect Luc or MDH from heat-induced aggregation. Wild-type PsHsp18.1 protects Luc at a molar ratio of 4:1 and MDH at a ratio of 2:1 (sHSP:substrate).

BIOCHEMISTRY

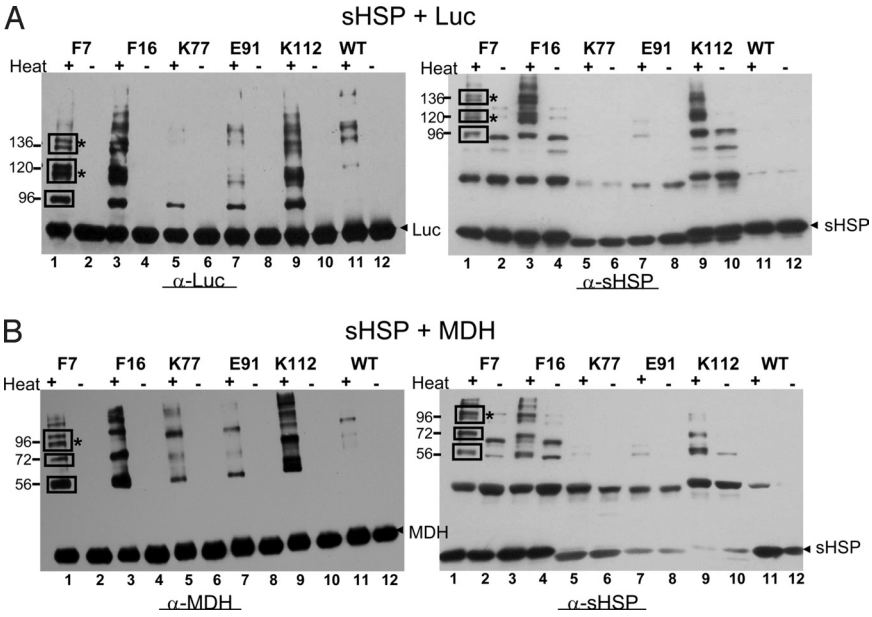

Fig. 3. PsHsp18.1 cross-links to MDH and Luc only under substrate denaturing conditions. The indicated Bpa variant or wildtype PsHsp18.1 were heated (+, odd numbered lanes) or not (−, even numbered lanes) in the presence of Luc (*A*) or MDH (*B*). After UV-cross-linking and SDS/PAGE, samples were immunoblotted using sHSP or substrate specific antisera for detection. Three prominent cross-linked species with MDH and Luc are detected with the N-terminal variants, F7 and F16, and are indicated with open boxes. Species marked with an asterisk have two cross-link products migrating very close to each other. These most likely differ by one sHSP. No cross-links are detected in lanes 11 and 12 which contain the control of wild-type PsHsp18.1 (no Bpa). The high molecular weight species in lane 11 in the anti-Luc and anti-MDH blots result from minor protein aggregation during incubation at high temperature. sHSP specific oligomers are seen in all lanes of the anti-sHSP blots. Positions of molecular markers are indicated.

The Majority of Bpa Variants Show Wild-Type Chaperone Activity. Chaperone activity of the Bpa variants was measured by their ability to protect the model substrates MDH and Luc from heat-induced aggregation. For MDH, wild-type or Bpa-substituted PsHsp18.1 was mixed with MDH at 1:1, 2:1, or 4:1 molar ratios (sHSP:MDH) and incubated for 120 min at 45 °C, conditions which lead to full aggregation of MDH in the absence of sHSP (20). Luc protection was tested at molar ratios of 3:1, 6:1, or 12:1 (sHSP:Luc) and incubated for 8.5 min at 42 °C. Luc is more heat-sensitive than MDH and aggregates completely under these conditions in the absence of sHSP (20). After incubation, soluble and pellet fractions were analyzed by SDS/PAGE.

All nine N-terminal arm variants fully protected MDH at a 1:1 molar ratio, which is as efficient as wild-type PsHsp18.1 (Fig. 2*B* and Table S1). In contrast, protection of Luc differed between these variants. Like wild type, F7, F8, F16, F19, F30, and F32 completely protected at a molar ratio of 4:1, sHSP:Luc, but protection by L27, F41 and F48 required a three-fold higher ratio of sHSP (12:1). This result may indicate that the native residues at the latter positions are essential for recognizing denaturing Luc, or that Bpa introduces steric constraints, preventing the N-terminal arm from accessing a conformation necessary for Luc binding. These observations indicate that there are differences in the way the sHSP recognizes and binds MDH compared with Luc. It is also interesting that the unstable oligomers formed by F16 and F19 both protected MDH and Luc as efficiently as wild type. Thus, oligomeric stability did not affect chaperone efficiency in these assays. The data further support the importance of the N-terminal arm in substrate recognition and indicate that different substrates are not recognized/protected equivalently.

Differential protection of the two substrates was also seen for Bpa variants in the α-crystallin domain (Fig. 2 and Table S1). Twelve of the 21 variants, including three with abnormal quaternary structure (K96, E102, and F113) protected both substrates similarly to wild-type. In contrast, K56 protected Luc like wild-type but was 50% as effective with MDH, and E79 showed the reverse behavior. Although E60 showed normal dodecameric behavior, it was only 50% as effective as wild type in protecting both substrates. None of the remaining six Bpa variants fully protected either substrate. These results further support differential interaction of substrates with sHSPs and indicate specific residues within the α-crystallin domain are critical for substrate protection, distinct from oligomer stability.

In the C-terminal extension, although I146 disrupted the dodecamer, it protected MDH and Luc as efficiently as wild type. E145 was 50% less efficient than wild type (on a molar basis) in protecting both substrates (Fig. 2*B*), despite having apparently normal dodecameric structure.

PsHsp18.1 Bpa Variants Cross-Link Substrate Only in sHSP-Substrate Complexes. We next tested the Bpa variants for ability to cross-link with substrate. sHSP-substrate interactions are observed when sHSP and substrate are heated together under substrate denaturing conditions. In the absence of heat, no interaction of sHSP with native substrate is observed (Fig. S1) (2, 20). Therefore, cross-linking of sHSP to substrate should be observed only after heat denaturation of substrate in the presence of sHSP. The 24 PsHsp18.1 Bpa variants that fully protected MDH, Luc or both were incubated with substrate either at room temperature or with heating, using 120 min at 45 °C for MDH and 8.5 min at 42 °C for Luc. The molar ratio of sHSP (monomer) to substrate was 2.4:1 for MDH and 4:1 for Luc. For wild-type PsHsp18.1 these ratios result in full protection of substrate and complete incorporation of both proteins into sHSP-MDH complexes (Fig. S1), although some residual sHSP dodecamer is seen with the sHSP-Luc complex (data not shown). For cross-linking the preformed sHSP-substrate complexes or unheated sHSP-substrate mixtures were subjected to UV irradiation at 365 nm for 20 min on ice. UV-cross-linking did not alter the behavior of sHSP, MDH, Luc or the sHSP-substrate complexes as assessed by SEC (Fig. S1). Cross-linked species were then identified by separation on SDS/PAGE followed by immuno-blotting with sHSP and substrate-specific antisera.

As shown in Fig. 3 for selected PsHsp18.1 Bpa variants, sHSP-MDH or sHSP-Luc cross-linked species are seen in the heated samples (odd-numbered lanes), but not in the unheated controls (even numbered lanes), demonstrating that PsHsp18.1 only interacts with substrate when the substrate is heat denatured. Multiple sHSP-substrate species are detected for both substrates. These correspond in apparent molecular weight to one, two, or more sHSP monomers cross-linked to one substrate molecule. Because Bpa only captures interactions within a few Å, covalently bound substrate must interact with the sHSP very near the site of Bpa incorporation. As expected, no cross-linked

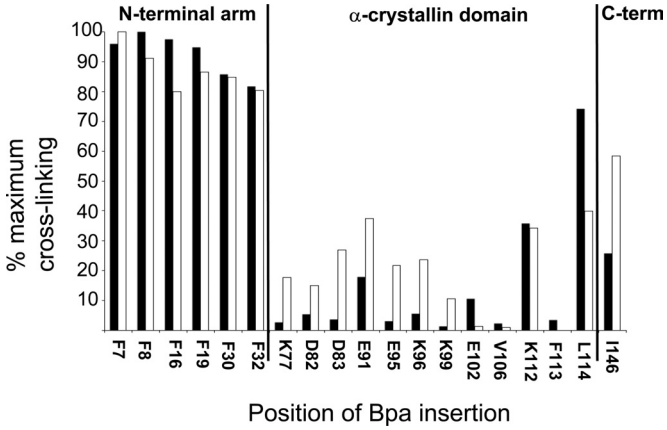

Fig. 4. Substrate cross-linking to PsHsp18.1 reveals major interactions with the N-terminal arm. Comparison of 19 Bpa variants which protected both MDH and Luc at wild-type molar ratios of sHSP:substrate. Intensity of cross-linked species is shown as a percentage maximum of F7 for MDH (white bars) and F8 for Luc (black bars).

products are seen with wild-type PsHsp18.1, which does not contain Bpa, although some aggregated higher molecular weight Luc and MDH bands are detected in the sample heated with wild-type protein.

In addition to species corresponding to sHSP cross-linked to substrate, species corresponding to sHSP cross-linked to itself are seen in both heated and unheated samples. This is expected since PsHsp18.1 is a dodecamer consisting of dimeric building blocks. Interestingly the intensity of sHSP multimers is reduced in the heated sample consistent with the Bpa cross-linking with the substrate rather than another molecule of sHSP (Fig. 3).

Substrates Preferentially Cross-Link to the N-Terminal Arm. The immunoblots in Fig. 3, and parallel analysis of the other Bpa variants, indicate that cross-linking occurs with different efficiencies across the protein, reflecting the extent of substrate interaction with specific sites on the sHSP. To quantify this difference in sHSP-substrate interaction, the cross-linked mixtures were separated by SDS/PAGE, stained with Coomassie blue (Fig. S2 *A* and *B*), and the amount of cross-linked species quantified. Quantification of cross-linked bands was reproducible with an estimated error of 2%–5% (*Materials and Methods*). Fig. 4 shows the results for only those 19 variants that fully protected both Luc and MDH, expressed as a percentage of the position exhibiting maximum cross-linking for either substrate (F7 for MDH, F8 for Luc). Strikingly, the N-terminal arm shows the strongest cross-linking to both substrates. The only other positions that show >30% cross-linking to both substrates are K112 and L114, in or next to β7 of the α-crystallin domain, which is close to the N-terminal arm in the TaHsp16.9 structure (10).

Contacts of the N-terminal arm with MDH were further examined using the three additional variants, L27, F41 and F48, which fully protect MDH, but not Luc (Table S1). Interestingly, L27 and F41 showed approximately 80%, while F48 showed <40% maximum cross-linking, perhaps related to proximity to core α-crystallin domain (Table S1 and Fig. S2*C*). Altogether, the results clearly demonstrate that the PsHsp18.1 N-terminal arm is the major structural feature involved in substrate contacts.

Interactions of PsHsp18.1 with MDH and Luc Are Not Identical. The cross-linking data in Fig. 4 also demonstrate that the interaction pattern of MDH and Luc with the sHSP is detectably different. There is a small, but significant difference in the N-terminal arm at position F16, which interacts more strongly with Luc than MDH. In the α-crystallin domain cross-linking of MDH to variants at K77 through K99 is significantly stronger than results with Luc, which shows almost no cross-linking in this region (with the exception of <20% reaction with E91). L114 in β7 shows an approximate 2-fold greater cross-linking to Luc than MDH, while for the C-terminal residue I146 the extent of interaction is reversed. These differences in cross-linking, along with the fact that certain specific Bpa variants in both the N-terminal arm and α-crystallin domain can fully protect MDH or Luc, but not both substrates (described above), are consistent with the interpretation that there is no single surface of the sHSP involved in substrate binding.

Discussion

We have identified specific positions of a sHSP that interact directly with partially denaturing substrates, providing insights into how these ubiquitous chaperones can bind and protect diverse proteins. Site-specific incorporation of the photocross-linker Bpa at multiple positions in each sHSP domain has allowed us to pinpoint sHSP-substrate interaction sites, even though the sHSP-substrate complex is large and heterogeneous. Bpa is a zero-length cross-linker that can incorporate into virtually any C-H or N-H bond, and is therefore well-suited for testing chaperone interactions with denaturing substrates, which are expected to involve hydrophobic contacts. Our results clearly show that the N-terminal arm of PsHsp18.1 forms multiple contacts with both MDH and Luc during heat denaturation (Figs. 3 and 4). Although an essential function for the sHSP N-terminal arm in substrate protection has been proposed (2, 20–23, 28), our data provide direct evidence that the N-terminal arm binds substrate. We also show that regions of the α-crystallin domain and C-terminal extension form substrate specific cross-links, but at a lower intensity compared with those of the N-terminal arm (Fig. 4). We interpret the difference in cross-linking intensity across the sHSP as indicating that there are differences in affinity of substrates to different sites on the protein. The combination of multiple N-terminal binding sites appears to form the highest affinity interaction with substrate compared with other regions of the sHSP. Previous studies have suggested there are both high and low affinity substrate binding sites on sHSPs (25, 29). Our results complement this idea by demonstrating that sHSPs can bind to substrate through a plastic interaction surface. Thus, unlike Hsp90, Hsp70, and GroEL, which have defined substrate binding sites (30, 31), the sHSPs engage the entire N-terminal arm, and other regions of the protein for substrate binding, which no doubt contributes to their high efficiency of substrate protection.

While the importance of the N-terminal domain is unambiguous, defining substrate interactions with the α-crystallin domain is more complex. Previous studies of hydrophobic probe binding and chemical cross-linking indicated that the β3-β5 region of the α-crystallin domain participates in substrate binding (see Fig. 1) (14, 24, 25, 32). Our experiments probed this region with Bpa introduced at positions K72, K77, E79, D82, D83, and Q87. While MDH formed cross-links with this region, Luc showed little or no interaction. Differential interaction of MDH and Luc with the α-crystallin domain was also observed in experiments using chimeric sHSPs in which identity of the α-crystallin domain affected protection of MDH, but not of Luc (20). Even for MDH, however, the intensity of cross-linked species was low in this region, despite the fact that introducing Bpa at these sites would increase the surface hydrophobicity of the sHSP and thereby increase potential for interactions with hydrophobic substrate surfaces. One limitation to using Bpa, a somewhat bulky probe, was the inability to incorporate it at number of sites in the α-crystallin domain (Fig. 1), even at positions predicted to be surface exposed in the dodecamer (Fig. S3). Therefore, some regions of the α-crystallin domain are not

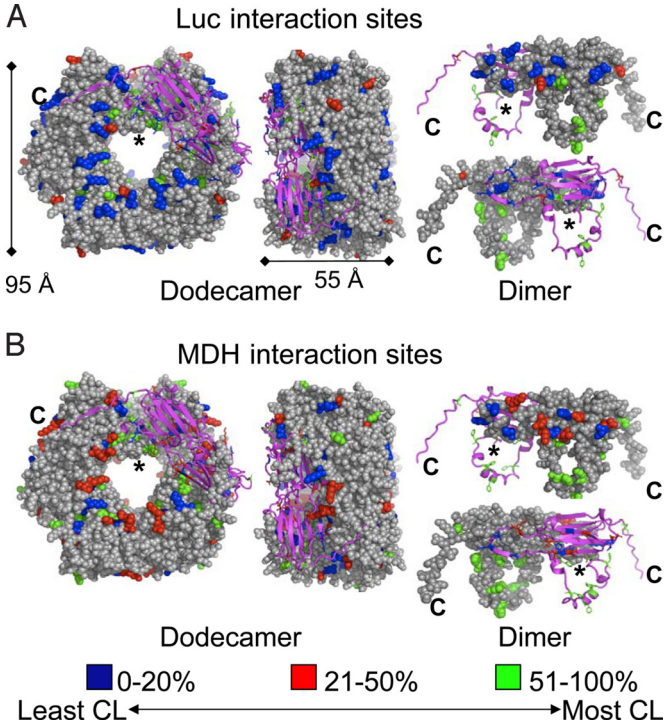

Fig. 5. MDH and Luc cross-linking results mapped to the PsHsp18.1 structure reveal that the main interaction regions are only fully exposed in the sHSP dimer. PsHsp18.1 Bpa variants protecting each substrate equivalently to wild-type were used for this analysis. Cross-linking results for Luc and MDH are mapped onto the space-filled models of PsHsp18.1 oligomer and dimer.

well-sampled by this method. However, the strongest interactions with the α-crystallin domain that were detected in our experiments occurred in or near β7 (K112 and L114). In TaHsp16.9, residues in the resolved N-terminal arms are in close proximity to β7, suggesting that strong interactions with this part of the α-crystallin domain reflect interactions with the N-terminal arm. While β7 has been proposed to be a potential substrate binding site, binding at β7 had not been detected experimentally (10). It is also very interesting that β7 contains a highly conserved Arg residue (R116 in PsHsp18.1), which is the site of mutations leading to different genetic diseases in humans (33, 34). Whether the effect of these mutations in vivo is linked to altered substrate interactions, as opposed to many other possible effects, remains to be determined.

Mapping the substrate cross-linking results onto the PsHsp18.1 model structure highlights another critical aspect of the sHSP chaperone mechanism (Fig. 5). The strongest cross-linking sites for both substrates are poorly accessible in the sHSP dodecamer. The N-terminal sites are even less accessible than in the model, considering that another approximately 27,000 Da of unresolved N-terminal arm residues must be accommodated in the central "hole", and are calculated to occupy essentially all of that space. Thus, substrate interactions with the N-terminal arm require extensive structural rearrangement of the dodecamer. It has been demonstrated that at substrate denaturing temperatures the equilibrium between the oligomeric and dimeric form of PsHsp18.1 and a number of other sHSPs is shifted toward the dimer (2, 10), suggesting this is the substrate-binding species. For other sHSPs increased temperatures result in more rapid subunit exchange, which would also facilitate binding to a suboligomeric species (35, 36). Because of difficulties in observing the sHSP-substrate interaction at high temperatures, substrate bound to a dimeric or other suboligomeric sHSP form has not been observed directly. Our demonstration of substrate binding to the N-terminal arm strongly supports the dimer as the active substrate binding form of PsHsp18.1. We can also rule out significant binding to the dimer interface, as E102 and V106 in β6 and K56 in β2, which are involved in this interface, show no significant cross-linking to either substrate (Fig. 4 and Table S1). This result indicates that monomers do not act as a major substrate-binding species. I146 of the C-terminal extension also interacts with both Luc and MDH, most likely because the C-terminal tail is free in the dimeric form of the sHSP.

Like the ATP-dependent chaperones GroEL, Hsp70 and Hsp90, sHSPs are believed to recognize and bind hydrophobic patches exposed on partially denatured proteins. However, unlike these other chaperones, which have distinct substrate binding regions, we can conclude that sHSPs rely on multiple contact sites distributed throughout the protein to protect substrates from irreversible aggregation. It is notable that the N-terminal arm of the sHSPs, apparently so critical to substrate interactions, represents an extensive, intrinsically unstructured domain (9, 10, 28, 37). A considerable body of evidence indicates that intrinsically unstructured regions of proteins play key roles in protein–protein interactions (38, 39). Interestingly, in contrast to coupled binding and folding of intrinsically disordered proteins (38, 39), hydrogen-deuterium exchange studies of the sHSP-substrate complex show that the N-terminal arm remains unstructured when bound to substrate (11). The observation that the substrate-bound N-terminal arm does not assume stable secondary structure is similar to recent observations of other proteins in which intrinsically disordered domains bind to interacting partners without a disorder-to-order transition (40). We propose that structural disorder allows the N-terminal arm to present a variable and flexible ensemble of clusters of hydrophobic residues that can interact with diverse geometries of hydrophobic patches on unfolding proteins. This ability to present multiple binding site conformations makes sHSPs highly effective at interacting efficiently to protect a wide range of critical cellular proteins.

Materials and Methods

Protein Expression and Purification. PsHsp18.1 single site mutants were generated using the Strategene quick change method (Stratagene) using a plasmid containing PsHsp18.1 with a C-terminal Strep tag (36). An amber stop codon was introduced at the desired position for Bpa incorporation and the mutant construct was transformed into BL21 *E. coli* cells along with the pSup-BpaRS-6TRN plasmid which was a generous gift from Dr. Peter Schultz (Scripps Institute, CA) (24). *E. coli* cells were grown in 2XYT media containing 1 mM Bpa (Bachem Americas, Inc.) and purified to >95% homogeneity by conventional methods (27). Protein concentrations were determined using the Bio-Rad protein assay (Bio-Rad Laboratories). The expected molecular masses of all Bpa variants were confirmed by mass spectrometry.

Size Exclusion Chromatography (SEC). Dodecameric stability of PsHsp18.1 Bpa variants at room temperature was assessed by applying 100 μL of 12 μM protein onto a TSKgel G5000PWxL column (Tosoh Biosciences) at a flow rate of 1 mL/min with a mobile phase of 25 mM Na phosphate, 150 mM KCl, pH 7.4. SHSP-substrate complexes were made by incubating 12 μM each of PsHsp18.1 Bpa variants with 3 μM Luc for 8.5 min at 42 °C or 5 μM MDH for 120 min at 45 °C. Complexes were cooled on ice and centrifuged for 15 min at 13,000 rpm. One hundred microliters of complex species was loaded on the column using buffers and flow rate specified above. A cross-linked sHSP-susbtrate complex was also analyzed to verify that the size and shape of the complex was the same after photo cross-linking.

Aggregation Protection Assay. To determine chaperone efficiency of PsHsp18.1 Bpa variants, 2 μM of Luc (recombinant *Photinus pyralis* luciferase, 62-kDa monomer from Promega) or 6 μM pig heart mitochondrial MDH, 33-kDa monomer (active form is dimeric) (Roche) were incubated at 8.5 min at 42 °C or 120 min at 45 °C, respectively, with the indicated ratios of sHSP. Substrate solubility was assayed as described in ref. 20.

Photoactivated Cross-Linking. Cross-linking reactions were performed on ice in 96 well microtiter plates with 50 μL preformed sHSP-substrate complex in 25

mM HEPES, 150 mM KCl, and 5 mM $MgCl_2$. Samples were irradiated at 365 nm using a handheld UV lamp (Model UVL-56, UVP). Sample irradiation time was optimized by testing irradiation times between 30 sec and 60 min. The relative intensity of cross-linking of the different Bpa variants was the same when the irradiation was performed at 2 min or at 20 min, as assessed by Western blot analysis (data not shown, Fig. 3). A 20-min cross-linking time was chosen because it produced sufficient cross-linked material to visualize and more accurately quantify on Coomassie blue-stained gels (see below). Longer cross-linking times increased the appearance of molecular weight species representing multiple sHSP linked to substrate without enhancing the well-resolved species predicted to contain one, two, or three sHSP monomers. sHSP and substrate mixed at the same ratio but incubated at room temperature for an equivalent time before cross-linking served as the controls. Samples were separated on 4%–20% SDS/PAGE. sHSP-substrate cross-linked species were identified by immunoblotting using sHSP and substrate specific antisera.

Quantifying Cross-Linked Products. Cross-linked mixture was resolved by 4%–20% SDS/PAGE and visualized by Coomassie Blue staining. The dominant cross-linked species as indicated in Fig. S2 was quantified using LI-COR software on an Odyssey imager (LI-COR Corp.). The highest measured cross-linked species, F7 for Luc and F8 for MDH, was set at 100% and the remaining variants are reported as a percentage for each substrate. PsHsp18.1 F32 variant served as an internal control on each gel. Each sample was run in triplicate and an average was used to calculate the % maximum. Estimated error was between 2% to 5%.

Molecular Modeling. A homology model of PsHsp18.1 monomer was generated using the protein fold recognition server, Homology/analogy Recognition Engine (41). The first 11 N-terminal residues are not included in the model. The PsHsp18.1 dodecamer was modeled based on TaHsp16.9 (PDB: 1GME) using Coot (42). Models were visualized and figures were prepared using MacPyMOL (http://www.pymol.org).

ACKNOWLEDGMENTS. We thank Peter Schultz at Scripps Institute for the generous gift of pSup-BpaRS-6TRN plasmid, Sue Roberts for help with molecular modeling, and Eman Basha and Vahe Bandarian for critical reading of the manuscript. This work was supported by National Institutes of Health Grant RO1-GM042762.

1. Liberek K, Lewandowska A, Zietkiewicz S (2008) Chaperones in control of protein disaggregation. *EMBO J* 27:328–335.
2. van Montfort R, Slingsby C, Vierling E (2001) Structure and function of the small heat shock protein/alpha-crystallin family of molecular chaperones. *Adv Protein Chem* 59:105–156.
3. Clark JI, Muchowski PJ (2000) Small heat-shock proteins and their potential role in human disease. *Curr Opin Struct Biol* 10:52–59.
4. Sun Y, MacRae TH (2005) The small heat shock proteins and their role in human disease. *FEBS J* 272:2613–2627.
5. Sharp P,S et al. (2008) Protective effects of heat shock protein 27 in a model of ALS occur in the early stages of disease progression. *Neurobiol Dis* 30:42–55.
6. Holmoy T, Vartdal F (2007) The immunological basis for treatment of multiple sclerosis. *Scand J Immunol* 66:374–382.
7. Olsen A, Vantipalli MC, Lithgow GJ (2006) Using *Caenorhabditis elegans* as a model for aging and age-related diseases. *Ann N Y Acad Sci* 1067:120–128.
8. Haslbeck M, Franzmann T, Weinfurtner D, Buchner J (2005) Some like it hot: The structure and function of small heat-shock proteins. *Nat Struct Mol Biol* 12:842–846.
9. Kim KK, Kim R, Kim SH (1998) Crystal structure of a small heat-shock protein. *Nature* 394:595–599.
10. van Montfort RL, Basha E, Friedrich KL, Slingsby C, Vierling E (2001) Crystal structure and assembly of a eukaryotic small heat shock protein. *Nat Struct Biol* 8:1025–1030.
11. Cheng G, Basha E, Wysocki VH, Vierling E (2008) Insights into small heat shock protein and substrate structure during chaperone action derived from hydrogen/deuterium exchange and mass spectrometry. *J Biol Chem* 283:26634–26642.
12. Wintrode PL, Friedrich KL, Vierling E, Smith JB, Smith DL (2003) Solution structure and dynamics of a heat shock protein assembly probed by hydrogen exchange and mass spectrometry. *Biochemistry* 42:10667–10673.
13. Mogk A, Deuerling E, Vorderwulbecke S, Vierling E, Bukau B (2003) Small heat shock proteins, ClpB and the DnaK system form a functional triade in reversing protein aggregation. *Mol Microbiol* 50:585–595.
14. Lee GJ, Roseman AM, Saibil HR, Vierling E (1997) A small heat shock protein stably binds heat-denatured model substrates and can maintain a substrate in a folding-competent state. *EMBO J* 16:659–671.
15. Franzmann TM, Menhorn P, Walter S, Buchner J (2008) Activation of the chaperone Hsp26 is controlled by the rearrangement of its thermosensor domain. *Mol Cell* 29:207–216.
16. Mogk A, Deuerling E, Vorderwulbecke S, Vierling E, Bukau B (2003) Small heat shock proteins, ClpB and the DnaK system form a functional triade in reversing protein aggregation. *Mol Microbiol* 50:585–595.
17. Shashidharamurthy R, Koteiche HA, Dong J, McHaourab HS (2005) Mechanism of chaperone function in small heat shock proteins: Dissociation of the HSP27 oligomer is required for recognition and binding of destabilized T4 lysozyme. *J Biol Chem* 280:5281–5289.
18. Benesch JL, Ayoub M, Robinson CV, Aquilina JA (2008) Small heat shock protein activity is regulated by variable oligomeric substructure. *J Biol Chem* 283:28513–28517.
19. Sharma KK, Kaur H, Kumar GS, Kester K (1998) Interaction of 1,1′-bi(4-anilino) naphthalene-5,5′-disulfonic acid with alpha-crystallin. *J Biol Chem* 273:8965–8970.
20. Basha E, Friedrich KL, Vierling E (2006) The N-terminal arm of small heat shock proteins is important for both chaperone activity and substrate specificity. *J Biol Chem* 281:39943–39952.
21. Haslbeck M, et al. (2004) A domain in the N-terminal part of Hsp26 is essential for chaperone function and oligomerization. *J Mol Biol* 343:445–455.
22. Giese KC, Basha E, Catague BY, Vierling E (2005) Evidence for an essential function of the N terminus of a small heat shock protein in vivo, independent of in vitro chaperone activity. *Proc Natl Acad Sci USA* 102:18896–18901.
23. Ghosh JG, Shenoy AK, Jr, Clark JI (2006) N- and C-Terminal motifs in human alphaB crystallin play an important role in the recognition, selection, and solubilization of substrates. *Biochemistry* 45:13847–13854.
24. Sharma KK, Kumar GS, Murphy AS, Kester K (1998) Identification of 1,1′-bi(4-anilino)naphthalene-5,5′-disulfonic acid binding sequences in alpha-crystallin. *J Biol Chem* 273:15474–15478.
25. Ahrman E, Lambert W, Aquilina JA, Robinson CV, Emanuelsson CS (2007) Chemical cross-linking of the chloroplast localized small heat-shock protein, Hsp21, and the model substrate citrate synthase. *Protein Sci* 16:1464–1478.
26. Ryu Y, Schultz PG (2006) Efficient incorporation of unnatural amino acids into proteins in *Escherichia coli*. *Nat Methods* 3:263–265.
27. Lee GJ, Vierling E (1998) Expression, purification, and molecular chaperone activity of plant recombinant small heat shock proteins. *Methods Enzymol* 290:350–365.
28. Aquilina JA, Watt SJ (2007) The N-terminal domain of alphaB-crystallin is protected from proteolysis by bound substrate. *Biochem Biophys Res Commun* 353:1115–1120.
29. Sathish HA, Stein RA, Yang G, McHaourab HS (2003) Mechanism of chaperone function in small heat-shock proteins. Fluorescence studies of the conformations of T4 lysozyme bound to alphaB-crystallin. *J Biol Chem* 278:44214–44221.
30. Mayer MP, Bukau B (2005) Hsp70 chaperones: Cellular functions and molecular mechanism. *Cell Mol Life Sci* 62:670–684.
31. Horwich AL, Fenton WA, Chapman E, Farr GW (2007) Two families of chaperonin: Physiology and mechanism. *Annu Rev Cell Dev Biol* 23:115–145.
32. Sharma KK, Kaur H, Kester K (1997) Functional elements in molecular chaperone alpha-crystallin: Identification of binding sites in alpha B-crystallin. *Biochem Biophys Res Commun* 239:217–222.
33. Vicart P, et al. (1998) A missense mutation in the alphaB-crystallin chaperone gene causes a desmin-related myopathy. *Nat Genet* 20:92–95.
34. Litt M, et al. (1998) Autosomal dominant congenital cataract associated with a missense mutation in the human alpha crystallin gene CRYAA. *Hum Mol Genet* 7:471–474.
35. Liu L, Ghosh JG, Clark JI, Jiang S (2006) Studies of alphaB crystallin subunit dynamics by surface plasmon resonance. *Anal Biochem* 350:186–195.
36. Friedrich KL, Giese KC, Buan NR, Vierling E (2004) Interactions between small heat shock protein subunits and substrate in small heat shock protein-substrate complexes. *J Biol Chem* 279:1080–1089.
37. Jiao W, Qian M, Li P, Zhao L, Chang Z (2005) The essential role of the flexible termini in the temperature-responsiveness of the oligomeric state and chaperone-like activity for the polydisperse small heat shock protein IbpB from *Escherichia coli*. *J Mol Biol* 347:871–884.
38. Tompa P, Csermely P (2004) The role of structural disorder in the function of RNA and protein chaperones. *FASEB J* 18:1169–1175.
39. Dyson HJ, Wright PE (2005) Intrinsically unstructured proteins and their functions. *Nat Rev Mol Cell Biol* 6:197–208.
40. Sigalov AB, Kim WM, Saline M, Stern LJ (2008) The intrinsically disordered cytoplasmic domain of the T cell receptor zeta chain binds to the Nef protein of simian immunodeficiency virus without a disorder-to-order transition. *Biochemistry* 47:12942–12944.
41. Bennett-Lovsey RM, Herbert AD, Sternberg MJ, Kelley LA (2008) Exploring the extremes of sequence/structure space with ensemble fold recognition in the program Phyre. *Proteins* 70:611–625.
42. Emsley P, Cowtan K (2004) Coot: Model-building tools for molecular graphics. *Acta Crystallogr D Biol Crystallogr* 60:2126–2132.